

Weakly Pinned Bose Glass vs. Mott Insulator Phase in Superconductors

Carsten Wengel¹ and Uwe Claus Täuber²

¹Department of Physics, University of California, Santa Cruz, California 95064

²Department of Physics — Theoretical Physics, University of Oxford, 1 Keble Road, Oxford OX1 3NP, U.K.
and Linacre College, St. Cross Road, Oxford OX1 3JA, U.K.

(October 6, 2018)

We study the properties of the Bose glass phase of localized flux lines in irradiated superconductors near the matching field B_Φ . Repulsive vortex interactions destroy the Mott insulator phase predicted to occur at $B = B_\Phi$. For ratios of the penetration depth to average defect distance $\lambda/d \leq 1$ remnants of the Mott insulator singularities remain visible in the magnetization, the bulk modulus, and the magnetization relaxation, as B is varied near B_Φ . For $\lambda \geq d$, the ensuing weakly pinned Bose glass is characterized by a soft Coulomb gap in the distribution of pinning energies.

PACS numbers: 74.60.Ge, 05.60.+w

For the application of high- T_c (type II) superconductors in external magnetic fields, an effective flux pinning mechanism is essential in order to minimize the resistive losses through Lorentz-force induced vortex motion. Specifically, columnar defects, i.e., linear damage tracks in the material caused by heavy-ion irradiation, have emerged as very effective pinning centers [1]. For such systems, a continuous vortex localization transition at T_{BG} from an entangled flux liquid to a disorder-dominated Bose glass phase was predicted [2,3], and subsequently found in experiment [1]. In addition, it was suggested that when the vortex and defect densities are equal, each flux line would be attached to one pin, leading to a Mott insulator phase within the Bose glass [3]. Recent measurements of the magnetization relaxation rate at low temperatures [4,5], and of the reversible magnetization itself [6,7], have been interpreted as signatures of this Mott insulator, and inspired further theoretical investigations [8–10]. Yet so far, the influence of the repulsive vortex interactions, whose range is set by the London penetration depth λ , has not been carefully studied.

The aim of this Letter is to explore numerically how the repulsive vortex forces affect the predicted Mott insulator as the magnetic field B is varied near the matching field B_Φ . Using a *random* defect distribution with average defect distance d , we extend earlier work which was limited to $B \ll B_\Phi$ [11]. Our findings are: 1) At B_Φ the Mott insulator, which is characterized by a *hard* gap Δ in the distribution of pinning energies $g(e)$ near the chemical potential μ , exists only for extremely short-range interactions $\lambda/d \rightarrow 0$ (Fig. 1, left inset); with increasing $\lambda < d$ the gap quickly fills and, therefore, the Mott insulator is destroyed (Fig. 1, right top inset). For long-range interactions $\lambda > d$ a *soft* Coulomb gap [12] described by $g(e) \propto |e - \mu|^{s_{\text{eff}}}$ emerges with an effective gap exponent s_{eff} (Fig. 1, bottom inset). 2) By measuring the reversible magnetization and the effective IV exponent, which is related to the magnetization relaxation rate, we are able to explain experimental results [4–7] as *remnants* of the Mott insulator for $\lambda < d$, but *not* as true signatures

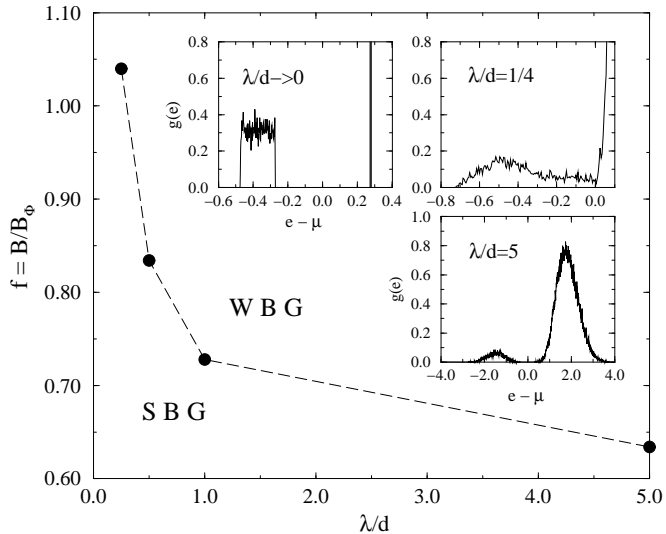


FIG. 1. SBG / WBG crossover line (see text) vs. λ/d . The insets show the pinning energy distribution $g(e)$ vs. $e - \mu$ for $\lambda/d \rightarrow 0$ (left), $\lambda/d = 1/4$ (right top) and $\lambda/d = 5$, all at B_Φ .

of this distinct thermodynamic phase itself. 3) We can identify a crossover line (Fig. 1), discriminating between the strong Bose glass (SBG, with all vortices localized by defects) and the weak Bose glass (WBG, with vortex bundle pinning) [3,8].

The theoretical description of the Bose glass is based on the following free energy of N_V flux lines, described by their 2d trajectories $\mathbf{r}_i(z)$ as they traverse a sample of thickness L in a magnetic field $\mathbf{B} \parallel \hat{\mathbf{z}}$ [2,3],

$$\mathcal{F} = \int_0^L dz \sum_{i=1}^{N_V} \left\{ \frac{\tilde{\epsilon}_1}{2} \left(\frac{d\mathbf{r}_i(z)}{dz} \right)^2 + \frac{1}{2} \sum_{j \neq i}^{N_V} V[r_{ij}(z)] + \sum_{k=1}^{N_D} V_D[\mathbf{r}_i(z) - \mathbf{R}_k(z)] \right\}. \quad (1)$$

This consists first of an elastic line tension term, with tilt modulus $\tilde{\epsilon}_1$. The second term denotes the interaction energy of all vortex pairs (local in z), where $r_{ij} = |\mathbf{r}_i - \mathbf{r}_j|$

and $V(r) = 2\epsilon_0 K_0(r/\lambda)$ is the screened repulsive vortex potential, with the modified Bessel function $K_0(x) \propto -\log(x)$ as $x \rightarrow 0$, and $K_0(x) \propto x^{-1/2} \exp(-x)$ for $x \rightarrow \infty$. The energy scale is set by $\epsilon_0 = (\phi_0/4\pi\lambda)^2$. The last term describes N_D columnar pins ($\parallel \mathbf{B}$), modeled by z -independent square well potentials V_D with average spacing d , centered on randomly distributed positions $\{\mathbf{R}_k\}$. The typical defect radius is $c_k \approx 50\text{\AA}$, and related to the pinning strengths U_k via $U_k \approx (\epsilon_0/2) \log[1 + (c_k/\sqrt{2}\xi)^2]$ [3]. The ion beam dispersion induces a distribution of the U_k with width $w = \sqrt{\langle \delta U_k^2 \rangle}$.

The mathematical analysis of Eq. (1) exploits a mapping of the statistical mechanics of this free energy of directed lines to the quantum mechanics of two-dimensional bosons subject to point disorder [2,3]. Here, we focus on the ground states properties of Eq. (1) for $B \sim B_\Phi$ at zero temperature, which is a fair approximation for the Bose glass phase for $T < T_1 \approx 0.6 \dots 0.8 T_{\text{BG}}$. In this regime, thermal wandering of vortices can be neglected [3,11,13,14], and the vortices will essentially be straight which allows us to ignore the elastic energy. This leaves us with a static two-dimensional problem of N_V interacting “particles” and N_D defects. For computational reasons we represent our problem on an underlying triangular grid with N “lattice” sites and therefore $N - N_D$ interdefect sites (“interstitials”). The effective Hamiltonian then reads

$$\mathcal{H}_{\text{eff}} = \frac{1}{2} \sum_{i \neq j}^N n_i n_j V(r_{ij}) + \sum_{k=1}^{N_D} n_k t_k , \quad (2)$$

where $\{n_i = 0, 1\}$ represent the site occupation numbers. If we take $\xi = 10\text{\AA}$ and $c_0 = 50\text{\AA}$, we obtain for the “bare” defect pinning energies $t_k = -\langle U_k \rangle + w_k$, with $\langle U_k \rangle = 0.65$ and width $w = 0.1$ in units of $2\epsilon_0$. For simplicity we assume a flat distribution of pinning energies around its mean, $P(w_k) = \Theta(w - |w_k|)/2w$, where Θ denotes the step function. The simulations are performed by randomly distributing N_V vortices and N_D defects on the triangular grid and minimizing the total energy with respect to single-particle transfers, thereby obtaining pseudo-groundstates for the Hamiltonian (2) [15]. Our simulations are mostly carried out with $N = 1600$, $N_D = N/16 = 100$, using periodic boundary conditions. We study physical quantities as functions of the interaction range $\lambda/d = 1/4, 1/2, 1, 5$, and the filling fraction $f = N_V/N_D = B/B_\Phi$, in the interval $0.2 \leq f \leq 3$. All distances are given in units of the lattice constant a of the triangular grid. The lower limit for the interaction range is determined by $\lambda = a$, since even smaller values effectively correspond to $\lambda \rightarrow 0$. We typically take an average over 50 different realizations of the disorder.

We have compared our findings for $f \leq 0.6$ with those obtained in Ref. [11], where it was assumed that all vortices remain bound to defects, irrespective of the value of λ , and therefore continuously spaced random positions could be used. Indeed, we were able to reproduce the

previous results for filling fractions $f = 0.2$ and $f = 0.4$ quantitatively. We have also tried to render the artificial grid finer by keeping N_D constant and increase N from 1600 to 3600, the largest sample we could study, and did not detect any lattice dependence for both grid sizes. Hence, we believe that our results should be largely insensitive to the underlying lattice representation, and provide a fair approximation to a more realistic continuum description. Also, we could not find any significant finite-size effects when keeping $N = 3600$ and λ/d fixed and increasing N_D from 36 to 100 and 225.

A natural first question to ask is how many flux lines are depinned as a result of the vortex interactions, depending on the values of f and λ/d . Within the Bose glass one may discriminate between the SBG and the WBG, where the latter is characterized by a markedly reduced localization temperature T_{BG} and critical current J_c [3]. For $\lambda/d \ll 1$, the crossover between these regimes is expected to occur for $B \sim B_\Phi$ [8]. Once interactions become strong, the WBG will appear well below B_Φ . Fig. 1 shows the filling fraction f_{occ} at which 10 % of the vortices are depinned, as a function of λ/d , which we tentatively take as a criterion to define a crossover line between the SBG and WBG. One observes a rather strong dependence of this line on λ/d , which is shifted well below B_Φ as soon as $\lambda \approx d$. Only for $\lambda/d \leq 1/4$ does the line remain above B_Φ ; yet obviously this is a prerequisite for the Mott insulator phase to appear.

In order to see if the Mott insulator persists for a finite interaction range *and* a random distribution of pinning sites, we compute the single-particle density of states $g(e)$, i.e. the distribution of (interacting !) pinning energies, where $e_i = \sum_{j \neq i} n_j V(r_{ij}) + t_i$. For long-range interactions ($\lambda \gg d$) one expects a soft “Coulomb” gap in $g(e)$ at the chemical potential $e = \mu$, separating occupied ($e < \mu$) from empty ($e > \mu$) states; near μ , $g(e)$ should vanish according to $g(e) \propto |e - \mu|^{s_{\text{eff}}}$ [12,11]. In the limit $\lambda/d \rightarrow 0$, on the other hand, the Mott insulator phase at $f = 1$ is characterized by the appearance of a hard gap separating the occupied defect states at $e = -\langle U_k \rangle \pm w$ from the unoccupied states at $e = 0$ (Fig. 1, left inset). The right insets in Fig. (1) show $g(e)$ at $f = 1$ for $\lambda/d = 1/4$ (top) and $\lambda/d = 5$ (bottom). The bottom figure exhibits a wide Coulomb gap, which we also find (though narrower) for $\lambda/d = 1$.

The top inset, however, only shows a fairly flat density of states for the occupied sites, which is somewhat depleted for $e \approx \mu$, and rises sharply for $e \geq \mu$. The fact that all states below μ are *continuously* filled implies that even rather short-range interactions suffice to destabilize a distinct thermodynamic Mott insulator phase [9]. We have also looked at $\lambda/d = 1/8$ by increasing N to 3600, using only $N_D = 56$, whence $d = \sqrt{N/N_D} \approx 8$, and even here we still found some states in the vicinity of μ . We are therefore led to conclude that for the true Mott insulator to appear in this system with a *random* spatial distribution of pinning sites, a necessary condition is

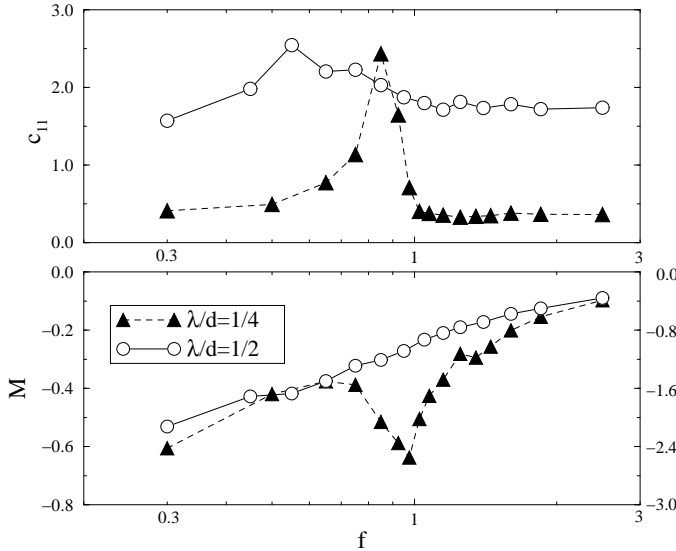


FIG. 2. Log-linear plots of the bulk modulus c_{11} (top) and the magnetization M (bottom) vs. f for $\lambda/d = 1/4$ (left scale in the bottom plot) and $\lambda/d = 1/2$ (right scale).

$\lambda \ll d$. We speculate that for a more regular array of columnar defects [16], the Mott insulator at $T = 0$ may persist to considerably larger interaction ranges [9].

Next, we have determined the chemical potential μ as a function of f , i.e. the $H(B)$ curve, defining $\mu = (e_{\max} + e_{\min})/2$ with e_{\max} the maximum site energy of the occupied states, and e_{\min} the minimum of the unoccupied site energies, and then averaging over disorder [12]. From this we obtain the bulk modulus of the system via $c_{11} = \partial\mu/\partial f = N_D \partial\mu/\partial N_V$. A divergence of c_{11} at B_Φ would indicate the appearance of the Mott insulator, which is incompressible (adding another vortex costs an energy Δ) and in this respect similar to the Meissner state. Correspondingly, its signature should be a sharp jump in μ at $f = 1$ [for $\lambda \rightarrow 0$ the height of this jump is given by the hard gap $\Delta = \langle U_k \rangle$ in $g(e)$]. Fig. 2 (top) shows that while the divergence is smeared out already for short-range interactions ($\lambda/d = 1/4$), yet a quite pronounced peak in c_{11} remains, shifted downwards to $f \approx 0.85$. For larger interaction range ($\lambda/d = 1/2$) the jump of μ is displaced to even smaller f (≈ 0.55) and less marked; for $\lambda \geq d$, the bulk modulus becomes essentially constant over the entire range of f . In both cases depicted here, the location of the peak in c_{11} coincides with that value of f at which a sizeable number of vortices actually leave the defect sites. The fact that the average bulk modulus is enhanced for larger λ is simply an energetic effect, since a vortex entering the system has to overcome a higher energy barrier due to the interactions. The behavior of c_{11} confirms again that no true Mott insulator exists even for relatively short-range interactions $\lambda/d = 1/4$ or $1/2$. We do observe, though, a distinctive "lock-in" structure for $\lambda/d < 1$, which completely disappears for $\lambda/d \geq 1$.

In order to make further contact with experiments,

we measured the total energy G , which yields the reversible magnetization via the thermodynamic relation $M = -\partial G/\partial B \propto -N_V^{-1} \partial G/\partial f$. Fig. 2 (bottom) depicts M as a function of f on a log-linear plot for $\lambda/d = 1/4$ and $\lambda/d = 1/2$. The data for $\lambda/d = 1/4$ show a pronounced minimum in M at $f \approx 1$, embedded in a slow logarithmic growth as f increases. The second plot for $\lambda/d = 1/2$ hardly displays any structure aside from a shallow dip near $f \approx 0.6$. This feature is completely absent for $\lambda/d \geq 1$, where only the $\log(\sqrt{f})$ increase remains, resembling the magnetization curve of an unirradiated superconductor [6,7,10]. The observed behavior of M at $\lambda/d = 1/4$ qualitatively agrees very well with recent measurements performed by van der Beek *et al.* in an irradiated BSCCO crystal [7], who find (at $T \approx T_1$) a pronounced dip in M centered near $B = B_\Phi$. The disappearance of this minimum in the experiments as $T \rightarrow T_{BG}^-$ may be at least partially due to the increase of the London penetration depth $\lambda(T)$, in addition to the entropic renormalizations studied in Ref. [10]. Our simulations cannot explain, however, the magnetization minima found at $f > 1$ in BSCCO tapes [6,17].

We would like to point out that the maximum in c_{11} occurs at *lower* values of f than the minimum in M (compare, e.g., our data for $\lambda/d = 1/4$), which can be understood as follows. Starting from the relation $M \propto B - H$, the bulk modulus may be written as $c_{11} \propto \partial H/\partial B \propto \text{const.} - \partial M/\partial B = \text{const.} + \partial^2 G/\partial B^2$; thus the maximum of c_{11} occurs at the location of the steepest negative slope in $M(B)$, which has to be at a smaller B than the minimum in M . Only in the "true" Mott insulator phase will the singularities both in c_{11} and M coincide at $B = B_\Phi$.

We now briefly return to the case of long-range interactions $\lambda/d > 1$, where a soft Coulomb gap appears in the distribution of pinning energies (r.h.s. inset in Fig. 1). Notice that the energetically favorable sites include both the defect and high-symmetry interstitial positions; thus, the original spatial randomness is in effect smoothed, and the gap exponent s_{eff} *increased* as compared to a situation where no interstitials are allowed [11]. At large f , a substantial fraction of the vortices will leave the pin positions, and as a consequence, Bose glass behavior can only be seen at low temperatures [14]. Yet, then the pinning via the repulsive forces exerted by neighbors that are still attached to columnar defects is very effective; we find that the potential minima are roughly equally deep and wide for all vortices in a given pseudo-ground state configuration, irrespective of the flux line occupying a defect or an interstitial site. This gives us confidence that the single-vortex density of states may indeed be used to infer low-current transport properties in the variable-range hopping regime [3,11].

In the localized Bose glass phase, vortex transport at low currents $J \ll J_c$ is expected to occur via variable-range hopping [3], in analogy with doped semiconductors [12]. In the spirit of the thermally-assisted flux flow

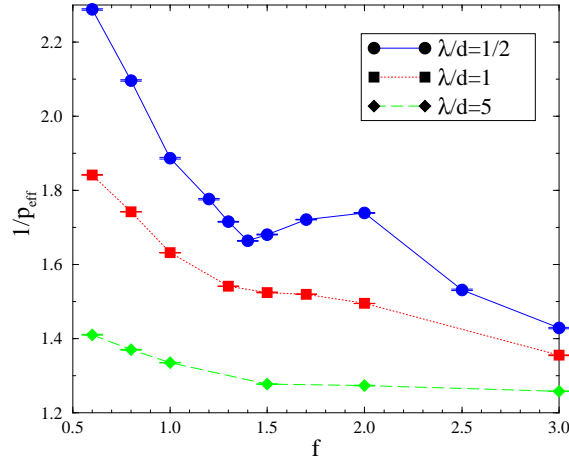


FIG. 3. Transport exponent $1/p_{\text{eff}}$ vs. f for $\lambda/d = 1/2, 1, 5$.

model, this leads to a highly nonlinear IV characteristics $\mathcal{E} = \rho_0 J \exp[-U_B(J)/k_B T]$, with effective (free) energy barriers that diverge according to $U_B(J) = U_0 (J_0/J)^{p_{\text{eff}}}$ as $J \rightarrow 0$. For short-range interactions, p_{eff} should be given by the 2d Mott variable-range hopping exponent $p_0 = 1/3$ [3]. Yet, once the vortex interactions become long-range, the emergence of a Coulomb gap in the distribution of pinning energies near μ leads to a considerable enhancement of flux pinning with effective exponents up to $p_{\text{eff}} \approx 0.7$, if $f = 0.1$ [11]. Such values for p_{eff} in the range between $1/3$ and 1 (as suggestive of the vortex half-loop excitations dominating for intermediate currents [3,11]) were found in recent magnetization relaxation experiments extending up to B_Φ [14].

We have calculated p_{eff} from the IV characteristics obtained by integrating over $g(e)$ for $e > \mu$ (see Ref. [11]). In Fig. 3 we plot p_{eff}^{-1} as a function of f for various values of λ/d . Remarkably, p_{eff} increases with growing vortex density for $f < 1$, as opposed to the earlier simulations where no interstitial positions were allowed and to the contrary a *decrease* with f was found, owing to the fact that the system had to accommodate with the underlying randomness [11]. Now, however, with favorable interstitial sites being available, the disorder effects are screened by the interactions as the vortex density increases. This leads to stronger correlations, and in fact more mean-field like behavior with larger values of p_{eff} as is apparently seen in experiment [14]. For $\lambda/d = 1/2$, we find a marked minimum in p_{eff}^{-1} at $f \approx 1.4$ (see Fig. 3) obviously due to a delicate interplay of disorder and correlation effects. Assuming that relaxation times are determined by the variable-range hopping energy barriers (vortex superkinks), $\log(t/t_0) \approx U_B(J)/k_B T$ [1], one finds for the magnetization relaxation rate $S = -dM/d \log t = -d \log J/d \log t = k_B T/p_{\text{eff}} U(J)$; therefore $S(B) \propto 1/p_{\text{eff}}(f)$. Hence, the minima in $S(B)$ near $B \approx 1.4B_\Phi$ detected by low-temperature relaxation

experiments on YBCO [4], and on a Tl-compound [5], might be explained by the maximum in p_{eff} we find with our simulations. At elevated temperatures, this structure should disappear quickly in this WBG regime.

In summary, we have investigated the Bose glass phase of flux lines localized by columnar defects near the matching field, taking the vortex interactions properly into account. For a random spatial distribution of pinning centers, the proposed Mott insulator phase is destabilized by the repulsive forces between the flux lines, but for a moderate interaction range $\lambda/d < 1$ interesting “lock-in” effects remain visible in the reversible magnetization, the bulk modulus, and the magnetization relaxation, which at least qualitatively explains a number of recent experiments. For larger $\lambda/d > 1$, the distribution of pinning energies displays a wide Coulomb gap, and sites available for variable-range hopping processes include both defect as well as high-symmetry interstitial positions.

We benefitted from discussions with M. Baumann, C.J. van der Beek, J.T. Chalker, J. Kötzler, L. Radzihovsky, and A.P. Young. C.W. acknowledges support from a NSF Grant DMR 94-11964 and U.C.T. through a European Commission TMR Grant ERB FMBI-CT96-1189.

- [1] For a recent review, see, e.g., G. Blatter *et al.*, Rev. Mod. Phys. **66**, 1125 (1994).
- [2] I. F. Lyuksyutov, Europhys. Lett. **20**, 273 (1992).
- [3] D. R. Nelson and V. M. Vinokur, Phys. Rev. Lett. **68**, 2398 (1992); Phys. Rev. B **48**, 13 060 (1993).
- [4] K. M. Beauchamp *et al.*, Phys. Rev. Lett. **75**, 3942 (1995).
- [5] E. R. Nowak *et al.*, Preprint (1995).
- [6] Q. Li *et al.*, Phys. Rev. B **54**, R788 (1996).
- [7] C. J. van der Beek *et al.*, Phys. Rev. B **54**, R792 (1996).
- [8] L. Radzihovsky, Phys. Rev. Lett. **74**, 4919 and 4923 (1995).
- [9] C. Reichhardt *et al.*, Phys. Rev. B **53**, R8898 (1996).
- [10] L. N. Bulaevskii *et al.*, Phys. Rev. Lett. **77**, 936 (1996).
- [11] U. C. Täuber *et al.*, Phys. Rev. Lett. **74**, 5132 (1995); U. C. Täuber and D. R. Nelson, Phys. Rev. B **52**, 16 106 (1995).
- [12] See, e.g., B.I. Shklovskii and A.L. Efros, *Electronic Properties of Doped Semiconductors* (Springer, Berlin, 1984).
- [13] L. Krusin-Elbaum *et al.*, Phys. Rev. B **53**, 11 744 (1996).
- [14] M. Baumann and J. Kötzler, priv. comm. (1996).
- [15] Details of this minimization procedure are described in Refs. [11,12], and further references therein.
- [16] See M. Baert *et al.*, Phys. Rev. Lett. **74**, 3269 (1995).
- [17] One possibility might be unspecified correlations in the spatial defect distribution in the sample.